American Journal of
Biomedical Science & Research

www.biomedgrid.com
ISSN: 2642-1747

Research Article

Comparison of Freeze-Drying and NaCL Particulate Leaching for Generating Surface and Bulk Porosity in Genipin-Crosslinked Gelatin Scaffolds: A Morphological Study

Emmanuella Rony[1], Adrian McCollum[2], Jesse Edwards[3*] and Jillian Pope[1,3*]

1Department of Chemistry, Florida A&M University, Tallahassee, FL 32307, USA

2Department of Biology, Florida A&M University, Tallahassee, FL 32307, USA

***Corresponding author:** Jesse Edwards & Jillian Pope, Department of Chemistry and Department of Biology, Florida A&M University, Tallahassee, FL 32307, USA Florida A&M University, Tallahassee, FL 32307, USA.

To Cite This article: *Emmanuella Rony, Adrian McCollum, Jesse Edwards* and Jillian Pope*, Comparison of Freeze-Drying and NaCL Particulate Leaching for Generating Surface and Bulk Porosity in Genipin-Crosslinked Gelatin Scaffolds: A Morphological Study. Am J Biomed Sci & Res. 2026 31(6) AJBSR.MS.ID.004104,* **DOI:** 10.34297/AJBSR.2026.31.004104

Received: August 04, 2026 **Published:** August 14, 2026

Abstract

Gelatin is an attractive nanoparticle matrix for drug delivery and imaging because it is collagen-derived, biodegradable, inexpensive, and of low antigenicity. Additionally, particle size is tunable through the desolvation process itself rather than through post-synthetic fractionation. Here, Type B bovine gelatin of two Bloom grades (75 and 225) was converted to nanoparticles by one-step and two-step desolvation with acetone at pH 2.5 and 60°C, crosslinked with glutaraldehyde, purified by dialysis against water, and characterized by dynamic light scattering with morphological confirmation by atomic force microscopy. Fluorescent preparations were made by labeling gelatin with Fluorescein-5-Isothiocyanate (FITC) in borate buffer before desolvation, and their association with A549 human lung adenocarcinoma cells was examined by confocal laser scanning microscopy after 24h. Size effects are reported as internally controlled ordinal comparisons rather than as absolute diameters. Two synthesis variables dominated the outcome. Bloom grade determined the direction of the size difference: in both the one-step and the two-step route, Bloom 225 gave larger particles than Bloom 75 under matched conditions, consistent with the higher average molecular weight of the higher-Bloom material. Crosslinker dose produced a secondary effect in the same series: doubling the glutaraldehyde charge from 54 to 108µL reduced particle size for both Bloom grades, consistent with network densification and contraction during crosslinking. Acidic pH favored smaller particles, and acetone addition beyond the point of maximal recovery broadened the distribution. Confocal imaging showed FITC-gelatin-derived fluorescence associated with A549 cells within 24h. Gelatin Bloom number is therefore a practical, purchasable handle on relative particle size, and the preparations show preliminary evidence of association with a lung epithelial carcinoma line relevant to inhaled and systemic delivery.

Keywords: Gelatin nanoparticles, Desolvation, Bloom number, Glutaraldehyde, A549, Cellular association

Introduction

Porous three-dimensional scaffolds provide temporary structural and biochemical support during tissue regeneration, and both the chemistry and the architecture of the scaffold influence cellular activity [1,2]. A scaffold intended to support cell ingrowth must be biocompatible, degrade on a timescale compatible with tissue formation, and present a pore network large enough for cell migration and nutrient transport while retaining sufficient surface area for attachment [3,4]. Pore size is not a free parameter: pores below roughly 100µm tend to fill with fibrous rather than mineralized tissue, whereas the 100–400µm window supports vascular invasion and osteoconduction, and further enlargement trades biological benefit against mechanical integrity [4,5]. Gelatin, obtained by thermal or chemical denaturation of collagen, is widely used for such scaffolds because of its biological origin,

biodegradability, commercial availability, and low cost [6,7]. Its triple-helix content, and hence gel strength, scales with Bloom number [6,8], and its abundant lysine and hydroxylysine ε-amino groups provide ready handles for crosslinking. The dominant limitation is rapid dissolution in aqueous media and poor resistance to endogenous gelatinases, which makes some form of stabilization mandatory [7].

Chemical crosslinkers address this directly but raise a residual-reagent problem: unreacted crosslinker and degradation products are the usual source of cytotoxicity rather than the network itself [9]. Genipin, an iridoid aglycone obtained by β-glucosidase hydrolysis of geniposide from Gardenia jasminoides, reacts with primary amines through nucleophilic attack at the C-3 position with ring opening, followed by secondary amine attack and oxidative dimerization, generating the characteristic blue pigment that makes the reaction self-reporting [10-12]. It is substantially less cytotoxic than glutaraldehyde in comparative in vitro assays [13,14]. DL-Glyceraldehyde, a fructose metabolite, crosslinks gelatin along the macromolecular chain through lysine residues and has been used for gelatin and chitosan microspheres [15,16]. Physical routes dehydrothermal treatment, UV irradiation, and microwave heating avoids reagent residues entirely by driving condensation between backbone carboxyl and amino groups, at the cost of poor control over crosslink density [17-20]. A separate set of operations generates porosity. Freeze-drying templates pores on the ice crystals formed during freezing, so that pore size is set by the freezing rate and thermal gradient rather than selected directly [21,22]. Particulate (porogen) leaching sets pore size by sieve fraction and porosity by porogen loading and has been applied to gelatin using NaCl [23,24]. The purpose of this work was to compare the two porogen routes under matched crosslinking conditions, and three crosslinking routes under matched porogen conditions, so that the two contributions to the final architecture can be separated. The study is deliberately limited to morphological and gravimetric endpoints.

Materials and Methods

Materials

Granular Type B gelatin (Bloom 75 and Bloom 225), genipin, DL-glyceraldehyde, and sodium chloride were obtained from Sigma-Aldrich (St. Louis, MO, USA). Acetone was of analytical grade. Deionized water was used throughout.

Gelatin Gel Preparation

Gelatin was weighed into polystyrene centrifuge tubes and dissolved in deionized water at 62°C at 12.5, 25.0, and 37.5% w/w. After complete dissolution, the solution was cast into polystyrene Petri dishes and held at 5°C to set.

Porous Scaffold Fabrication

Freeze-drying. Set gels were plunge-frozen in liquid nitrogen, held at −80°C, then lyophilized under vacuum with gradual shelf heating until the product temperature reached the shelf temperature. Particulate leaching. NaCl was sieved into 74–125, 125–180 and 180–355μm fractions. A salt bed was laid in the Petri dish, gelatin solution was poured over it, additional NaCl was distributed into the solution at a salt-to-gelatin weight ratio of about 4:1, and further crystals were applied to the free surface after the gel had set. Salt was leached with repeated changes of cold deionized water over 24hours, and the leached constructs were lyophilized as above. Completeness of salt removal was not verified instrumentally, for example by conductivity of the final rinse (Section 4.1). Both fabrication routes are summarized in (Table 1).

Table 1: Fabrication and assessment workflow. A single gelatin gel formulation was divided between two porogen routes (freeze-drying and NaCl particulate leaching) and three stabilization routes (genipin, DL-glyceraldehyde and microwave irradiation), so that porogen and crosslinker contributions to the final architecture could be separated.

1 — GEL FORMATION **Type B gelatin, Bloom 75 and 225, at 12.5 / 25.0 / 37.5% w/w · Dissolved at 62°C · Cast and Set at 5°C.**	
2A — Porogen: Freeze-Drying	**2B — Porogen: Particulate Leaching**
Plunge-freeze in liquid nitrogen → hold at −80°C → lyophilize under vacuum.	Sieved NaCl (74–125, 125–180, 180–355 μm) as a bed, within the gel and on the free surface → leach in cold water → lyophilize.
Pore space templated on the ice crystal population; pore size set indirectly by freezing rate.	Pore space templated on the salt crystals; pore size selected directly by sieve fraction.
3 — STABILISATION **genipin (2, 5, 15% w/w) · DL-glyceraldehyde · microwave (150°C, 16 bar, 2.45 GHz, 10–15 min)**	
4 — ASSESSMENT **SEM of surfaces and freeze-fractured cross-sections · gravimetric swelling, deionized water, 37°C, 24h**	

Chemical Crosslinking

Genipin: For solution crosslinking, gelatin was dissolved in deionized water at 62°C, genipin dissolved in acetone/water (2:1 v/v) was added, and the mixture was stirred at room temperature until the blue chromophore developed, then held at 5°C overnight. For crosslinking of preformed lyophilized films, 2.0g of film was immersed in 20mL acetone/water (2:1 v/v) containing genipin at 2, 5, or 15% w/w relative to gelatin and stirred for 15h at 4–10°C, followed by 10h at room temperature. Films were filtered, rinsed with cold acetone, and vacuum-dried overnight. DL-Glyceraldehyde: Lyophilized films were crosslinked with DL-glyceraldehyde at 2%

w/v in acetone/water at 5°C for 24h. A visible color change of the films accompanied crosslinking. Films were rinsed repeatedly with pre-cooled acetone and vacuum-dried for 24h.

Microwave-Assisted Crosslinking

Weighed pieces of lyophilized gelatin film were placed in microwave reactor vials with 2mL acetone as the polar heating medium and loosely covered to limit solvent loss. Samples were pre-stirred for 10min and irradiated for 10–15min at 150°C and 16 bar in a single-mode reactor (0–400 W, 2.45 GHz). Films were recovered and washed five times with 10mL acetone.

Scanning Electron Microscopy

Dried samples were mounted on stubs with double-sided tape, sputter-coated with gold, and imaged at 5– 15 keV accelerating voltage. Surfaces and freeze-fractured cross-sections were examined for each fabrication route. Pore architecture is described qualitatively from the micrographs; quantitative pore metrology was not performed (Section 4.1).

Swelling

Dry samples (2.5–3.0g) were weighed, immersed in 20 mL deionized water at 37°C for 24h, blotted on filter paper, and reweighed. Water uptake was calculated as W (%) = (W_w – W_d)/W_d × 100, where W_w and W_d are the wet and dry masses. Each condition was performed as three independent preparations, and the observations reported below are representative of those preparations; inferential statistics were not applied.

Results

Pore Architecture Depends on the Porogen, Not Only on the Polymer

Freeze-dried scaffolds showed only a small number of large openings at the free surface (Figure 1A), while freeze-fractured cross-sections revealed extensive interconnected porosity throughout the interior (Figure 1B). The architecture is consistent with ice templating: pore space reproduces the ice crystal population formed during freezing, and the surface in contact with the atmosphere sets as a comparatively dense skin.

Scaffolds prepared with NaCl incorporated into the gel and applied to the gel surface showed open pores in both locations after leaching (Figure 1C). Cross-sections showed larger, more clearly interconnected voids than the freeze-dried preparations (Figure 1D), and the constructs did not develop the membrane-like surface layer seen after freeze-drying alone. Salt removal was slow and required repeated water changes. Figure 1. Scanning electron micrographs of gelatin scaffolds by porogen route. (A) Freeze-dried, surface (5.0 kV, ×30). (B) Freeze-dried, freeze-fractured cross-section (15.0 kV, ×200). (C) NaCl particulate-leached surface (5.0 kV, ×100). (D) NaCl particulate-leached, freeze-fractured cross-section (15.0 kV, ×95). Instrument data bars are retained on each panel; scale bar 100 µm throughout. Freeze-drying generates interior porosity beneath a comparatively dense surface skin, whereas particulate leaching opens porosity at both the surface and in the bulk. Note that magnification differs between panels.

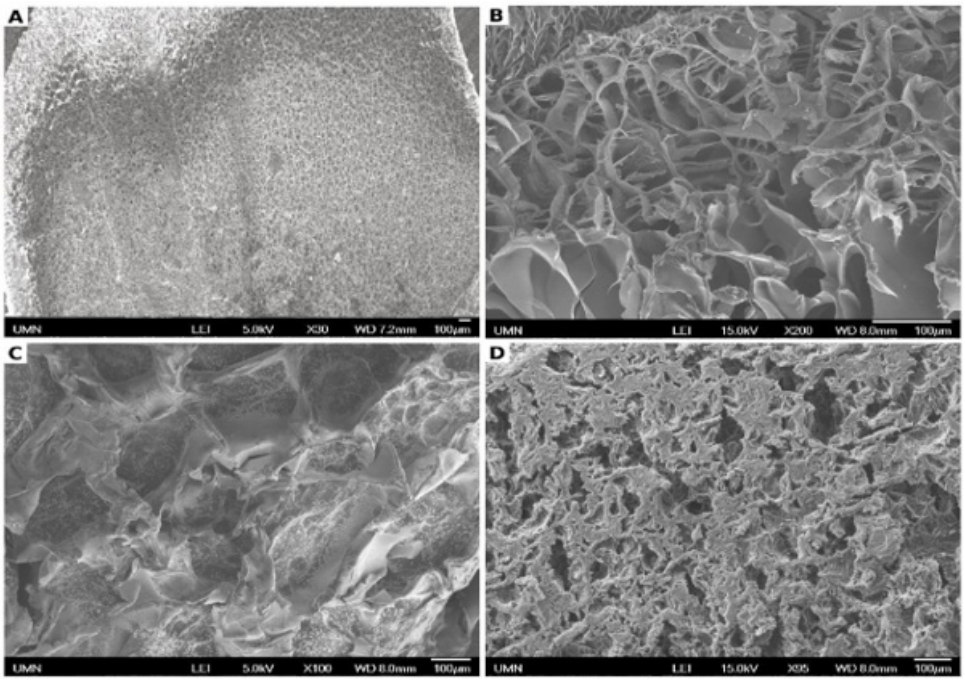

Figure 1: Scanning electron micrographs of gelatin scaffolds by porogen route. (A) Freeze-dried, surface (5.0 kV, ×30). (B) Freeze-dried, freeze-fractured cross-section (15.0 kV, ×200). (C) NaCl particulate-leached surface (5.0 kV, ×100). (D) NaCl particulate-leached, freeze-fractured cross-section (15.0 kV, ×95). Instrument data bars are retained on each panel; scale bar 100µm throughout. Freeze-drying generates interior porosity beneath a comparatively dense surface skin, whereas particulate leaching opens porosity at both the surface and in the bulk. Note that magnification differs between panels.

The dense skin observed after freeze-drying is a documented consequence of the cryogenic route rather than a feature specific to this preparation and is the reason ice templating is now routinely combined with a second pore-forming operation or with controlled directional freezing [21,22,25]. Because pore size in freeze-drying is set by freezing rate and thermal gradient, the same formulation frozen in liquid nitrogen and at a moderate subzero temperature will give different architectures, so the freezing protocol is part of the reported pore structure [21,22]. Particulate leaching, by contrast, decouples pore formation from thermal history and makes pore dimension a directly selected variable, which is the behavior observed here.

Genipin Outperformed DL-Glyceraldehyde, with a Usable Concentration Window

Genipin crosslinking was self-reporting: films developed the characteristic dark blue pigment within minutes at room temperature and deepened overnight at 5°C (Figure 2). Genipin-crosslinked films retained integrity in the 37°C water bath over 24h, whereas DL-glyceraldehyde-crosslinked films swelled substantially over the same period at the concentrations tested. Achieving comparable stabilization with DL-glyceraldehyde required a considerably larger reagent charge. Within the genipin series, 2% w/w was insufficient to hold the samples intact for the duration of the swelling test. At 15% w/w, the network was dense enough that pore openings appeared visibly occluded in the micrographs, which would be expected to impede cell migration, and the reagent cost at that loading is unattractive for scale-up. The 5% condition preserved both integrity and visible pore openings and is the condition carried forward (Figure 2).

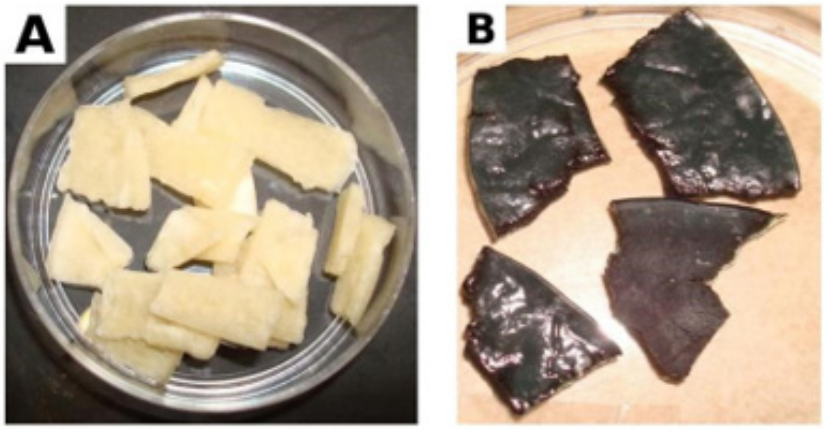

Figure 2: Genipin crosslinking is self-reporting. (A) Lyophilized gelatin films before crosslinking. (B) The same films after immersion in genipin solution and overnight reaction at 5°C, showing the dark blue chromophore formed on reaction of genipin with primary amines, which provides a visual indication that crosslinking has occurred.

Microwave Irradiation Produced Only Weak Crosslinking

Microwave-treated films showed only slight darkening and a small reduction in dimension and swelled markedly on 24h immersion. Under the conditions tested, the physical route did not stabilize the films to a degree comparable with either chemical crosslinker. This outcome is consistent with the underlying chemistry rather than with an instrument limitation. Thermal crosslinking of gelatin proceeds by condensation between backbone carboxyl and amino groups and requires removal of the water of condensation; classical dehydrothermal treatment therefore operates at 105–140°C under vacuum for hours to days [17,19,20]. Where microwave irradiation has been reported to assist collagen crosslinking, it has been applied in open or aldehyde-containing systems, the field accelerating an existing reaction rather than supplying a new one [26]. In a sealed microwave vial at 16 bars with acetone as the heating medium, the condensation water cannot be removed, and the equilibrium is unfavorable, so limited crosslink formation is the expected result. The observation is reported here because physical crosslinking is frequently proposed for gelatin, and the boundary condition is informative.

Discussion

Taken together, the results separate two contributions that are often conflated. Crosslinker identity and dose set the network density and therefore the aqueous stability and the extent to which pores remain open; the porogen sets where pore space is created. Neither substitute for the other: a well-crosslinked freeze-dried scaffold still presents a relatively closed surface, and a well-leached scaffold with insufficient crosslinking does not survive immersion at 37°C. The genipin concentration window observed here has a straightforward structural basis. Swelling is inversely related to crosslink density because shorter effective chain lengths between junctions restrict network expansion, so increasing genipin raises stability while simultaneously narrowing pore throats. The practical optimum is therefore not the most stable formulation but the least crosslinked formulation that survives the intended culture period. A systematic review of genipin-crosslinked gelatin scaffolds identifies concentrations of the order of 0.5% as optimal, more than an order of magnitude below the upper end of the range tested here, which is consistent with the observation that 15% w/w lies past the useful window [27].

Two developments since this work was performed bear on its interpretation. Gelatin Methacryloyl (GelMA) and enzymatic crosslinking with microbial transglutaminase have become the default comparators for gelatin scaffolds because they decouple gelation from crosslinking and permit photopatterning and printing [25,28]. Against those alternatives, genipin retains three practical advantages relevant to a low-cost fabrication route: no photoinitiator is required, the reaction reports its own progress optically, and the reagent is a natural product with a well characterized low cytotoxicity relative to aldehyde crosslinkers [13,14]. Establishing where each is preferable is a matter for direct comparison rather than for assertion.

Limitations

This study characterizes architecture and aqueous stability and does not extend to mechanical or biological performance. Pore dimensions are described from micrographs rather than quantified by image analysis, and interconnectivity is inferred from fracture surfaces rather than resolved tomographically. Crosslinking degree is expressed as reagent feed rather than as consumed amine content, so the genipin loadings reported here are not directly comparable with crosslink densities determined in other laboratories. Swelling in deionized water reports network density but is not a model of enzymatic degradation in vivo, for which crosslinker identity and degree alter degradation rate independently of swelling behavior [29]. Completeness of NaCl removal from the leached scaffolds was not verified instrumentally, so residual salt cannot be excluded as a contributor to the apparent porosity or to the measured water uptake. Gelatin Bloom grade was not resolved as an independent experimental factor: both Bloom 75 and Bloom 225 were used, but the scaffold observations are not separated by grade, and since triple-helix content and gel strength scale with Bloom number [6,8], this is a genuine gap. Data are drawn from three independent preparations and are presented without inferential statistics. The conclusions should therefore be read as a comparison of fabrication routes under matched handling conditions rather than as optimized design parameters.

Future Work

Three lines follow directly from these observations. First, quantitative pore metrology — mean Feret diameter and percentage porosity by threshold image analysis across multiple fields and independent scaffolds, with micro-computed tomography for interconnectivity — would allow the NaCl sieve fractions used here (74–355μm) to be related to realized pore dimensions, and thereby positioned against the 100– 400μm range currently associated with vascular invasion and osteoconduction [4,5,25]. A calibration between porogen fraction and realized pore size is the immediate priority and is obtainable from the existing sample set. Second, expressing crosslinking as consumed ε-amino content by TNBS or ninhydrin assay [30-32], supported for genipin by the absorbance of its blue chromophore near 590–600nm, would convert the 2/5/15% w/w reagent series into a crosslink-density series and permit direct comparison with published gelatin systems. Resolving Bloom grade as an explicit factor within the same design would add a full experimental dimension at modest cost, since both grades are already in hand.

Third, unconfined compression of hydrated scaffolds and collagenase-mediated degradation, followed by cell seeding with assessment of infiltration depth and viability, are required before these constructs can be evaluated as tissue-engineering scaffolds rather than as porous materials. Beyond the present system, the microwave result indicates that residue-free stabilization of gelatin is better pursued by dehydrothermal treatment under vacuum or by UV-mediated crosslinking, where the water of condensation can be removed [17-20]; and direct benchmarking of genipin against GelMA and enzymatic crosslinking would establish the conditions under which a self-reporting, photoinitiator-free natural crosslinker remains the preferable choice [25,29].

Conclusions

Under matched conditions, NaCl particulate leaching produced open porosity at both the surface and the interior of gelatin scaffolds, whereas freeze-drying alone produced interior porosity beneath a comparatively dense skin. Genipin stabilized gelatin films against 37°C immersion more efficiently than DL-glyceraldehyde on a reagent-mass basis, with an operating window bounded below by loss of integrity at 2% w/w and above by apparent pore occlusion at 15% w/w; 5% w/w was the practical compromise. Microwave irradiation in a sealed vessel did not achieve useful crosslinking, consistent with the requirement for removal of the water of condensation in thermal crosslinking. Combining moderate genipin crosslinking with porogen leaching is therefore the more promising of the routes examined, and the quantitative pore, crosslink-density and mechanical measurements set out in Section 4.2 are the next step toward usable design rules.

Author Contributions, Funding, Competing Interests and Data Availability

CRediT. Emmanuella Rony: investigation, formal analysis, visualization, writing the original draft. Jesse Edwards: conceptualization, methodology, supervision, resources, writing review and editing. Jillian Pope analysing data, writing review, and editing. Funding. Provided in part by the FAMU Chemistry Department and FAMU University Title II programs and a summer program with the University of Minnesota and the UCSB Materials Research Science and Engineering Center Summer. Research Program and a program affiliated with the Materials Research Facilities Network, DMR0819885 and DMR-0520415. Competing interests. The authors declare no competing financial or personal interests. Data availability. The micrographs and swelling records supporting this study are available from the corresponding author on reasonable request.

Acknowledgements

The freeze-drying, microwave and scanning electron microscopy work was carried out with the assistance of colleagues at the University of Minnesota and the University of California, Santa Barbara. The authors thank Dr. Frank Snowden (Deceased);

Dr. Ronald Siegel and members of his laboratory (Isha Koonar, Arum Kim and Dan Jung); Dr. Chun Wang and members of the Department of Biomedical Engineering; Marc von Keitz and Lindsey Jader of the Biotechnology Resource Center, St Paul campus, for assistance with lyophilization; Dr. Rebecca Cuellar of the Institute for Therapeutic Discovery and Development for training on the microwave synthesizer; and Dr. Anika Assata Odukale Edwards of the Materials Research Laboratory, University of California, Santa Barbara, for training on the scanning electron microscope. We would also like to thank Dr. Nelly Mateeva for her support.

References

1. Chen G, Ushida T, Tateishi T (2002) Scaffold design for tissue engineering. Macromol Biosci 2(2): 67–77.
2. Sahoo R, A Swaroop Sanket, Ananya Pattnaik, Swarnaprabha Pany, Sanghamitra Pradhan, et al. (2026) Designing of porous scaffolds for tissue engineering and regenerative medicine. J Mater Chem B 14(9): 2733-2773.
3. Hubbell JA (1995) Biomaterials in tissue engineering. Nat Biotechnol 13(6): 565–576.
4. Karageorgiou V, Kaplan D (2005) Porosity of 3D biomaterial scaffolds and osteogenesis. Biomaterials 26(27): 5474–5491.
5. Mukasheva F, Adilova L, Dyussenbinov A, Yernaimanova B, Abilev M, et al. (2024) Optimizing scaffold pore size for tissue engineering: insights across various tissue types. Front Bioeng Biotechnol 12: 1444986.
6. Bigi A, Panzavolta S, Rubini K (2004) Relationship between triple-helix content and mechanical properties of gelatin films. Biomaterials 25(25): 5675–5680.
7. Broderick EP, Damien MO Halloran, Yury A Rochev, Martin Griffin, Russell J Collighan, et al. (2005) Enzymatic stabilization of gelatin-based scaffolds. J Biomed Mater Res B Appl Biomater 72(1): 37–42.
8. Bigi A, Cojazzi G, Panzavolta S, Rubini K, Roveri N (2001) Mechanical and thermal properties of gelatin films at different degrees of glutaraldehyde crosslinking. Biomaterials 22(8): 763–768.
9. Ratcliffe JH, Hunneyball IM, Smith A, Wilson CG, Davis SS (1984) Preparation and evaluation of biodegradable polymeric systems for the intra-articular delivery of drugs. J Pharm Pharmacol 36(7): 431–436.
10. Djerassi C, Nakano T, James AN, Zalkow LH, Eisenbraun EJ, et al. (1961) Terpenoids XLVII: the structure of genipin. J Org Chem 26(4): 1192–1206.
11. Butler MF, Ng YF, Pudney PDA (2003) Mechanism and kinetics of the crosslinking reaction between biopolymers containing primary amine groups and genipin. J Polym Sci a Polym Chem 41(24): 3941–3953.
12. Liang HC, Chang WH, Lin KJ, Sung HW (2003) Genipin-crosslinked gelatin microspheres as a drug carrier for intramuscular administration: *in vitro* and *in vivo* studies. J Biomed Mater Res A 65(2): 271– 282.
13. Sung HW, Huang DM, Chang WH, Huang RN, Hsu JC (1999) Evaluation of gelatin hydrogel crosslinked with various crosslinking agents as bioadhesives: *in vitro* study. J Biomed Mater Res 46(4): 520– 530.
14. Ikada Y, Tabata Y (1998) Protein release from gelatin matrices. Adv Drug Deliv Rev 31(3): 287–301.
15. Vandelli MA, Pifferi G, Seghizzi R, Cameroni R (1995) Swelling behavior of gelatin microspheres crosslinked with DL-glyceraldehyde: the effect of the preparative factors. Pharm Pharmacol Lett 5: 116–119.
16. Griffini A, Vandelli MA, Seghizzi R, Mucci A, Pifferi G (1996) Pharmaceutical evaluation of gelatin microspheres crosslinked with DL-glyceraldehyde: determination of residuals of the preparation procedure. Pharm Pharmacol Lett 6:16–18.
17. Yannas IV, Tobolsky AV (1967) Crosslinking of gelatin by dehydration. Nature 215: 509–510.
18. Weadock KS, Miller EJ, Bellincampi LD, Zawadsky JP, Dunn MG (1995) Physical crosslinking of collagen fibers: comparison of ultraviolet irradiation and dehydrothermal treatment. J Biomed Mater Res 29(11): 1373–1379.
19. Haugh MG, Jaasma MJ, O Brien FJ (2009) The effect of dehydrothermal treatment on the mechanical and structural properties of collagen-GAG scaffolds. J Biomed Mater Res A 89(2): 363–369.
20. Esposito E, Cortesi R, Nastruzzi C (1996) Gelatin microspheres: influence of preparation parameters and thermal treatment on chemico-physical and biopharmaceutical properties. Biomaterials 17(20): 2009–2020.
21. O Brien FJ, Harley BA, Yannas IV, Gibson L (2004) Influence of freezing rate on pore structure in freezedried collagen-GAG scaffolds. Biomaterials 25(6): 1077–1086.
22. Haugh MG, Murphy CM, O Brien FJ (2010) Novel freeze-drying methods to produce a range of collagen– glycosaminoglycan scaffolds with tailored mean pore sizes. Tissue Eng Part C Methods 16(5): 887– 894.
23. Lee SB, Kim YH, Chong MS, Hong SH, Lee YM (2005) Study of gelatin-containing artificial skin V: fabrication of gelatin scaffolds using a salt-leaching method. Biomaterials 26(14): 1961–1968.
24. Kang HW, Tabata Y, Ikada Y (1999) Fabrication of porous gelatin scaffolds for tissue engineering. Biomaterials 20(14): 1339–1344.
25. Mohammad Hossein Mirmusavi, Vanessa SS Gonçalves, Christian Wischke (2025) Gelatin-based porous scaffolds: design concepts, production, and applications in precision regenerative medicine. Mater Today Bio 36: 102710.
26. Visser CE, Voute ABE, Oosting J, Boon ME, Kok LP (1992) Microwave irradiation and crosslinking of collagen. Biomaterials 13(1): 34–37.
27. (2019) Genipin-crosslinked gelatin scaffold in tissue engineering: a systematic review. Med Health 14(2): 1–16.
28. Yue K, Trujillo de Santiago G, Alvarez MM, Tamayol A, Annabi N, et al. (2015) Synthesis, properties, and biomedical applications of gelatin methacryloyl (GelMA) hydrogels. Biomaterials 73: 254–271.
29. Ozeki M, Tabata Y (2005) *In vivo* degradability of hydrogels prepared from different gelatins by various crosslinking methods. J Biomater Sci Polym Ed 16(5): 549–561.
30. Kale R, Bajaj A (2010) Ultraviolet spectrophotometric method for determination of gelatin crosslinking in the presence of amino groups. J Young Pharm 2(1): 90–94.
31. Arif MMA, Fauzi MB, Nordin A, Hiraoka Y, Tabata Y, et al. (2020) Fabrication of bio-based gelatin sponge for potential use as a functional acellular skin substitute. Polymers (Basel) 12(11): 2678.
32. Campiglio CE, Contessi Negrini N, Farè S, Draghi L (2019) Crosslinking strategies for electrospun gelatin scaffolds. Materials (Basel) 12(15): 2476.